

# The Chemical Nature of Surface Point Defects on MoO<sub>3</sub>(010): Adsorption of Hydrogen and Methyl

M. Chen,<sup>†</sup> C. M. Friend,<sup>\*,†</sup> and Efthimios Kaxiras<sup>‡</sup>

Contribution from the Department of Chemistry and Department of Physics and Division of Engineering and Applied Sciences, Harvard University, Cambridge, Massachusetts 02138

Received December 15, 1999. Revised Manuscript Received December 19, 2000

**Abstract:** We report density functional theory calculations using the Adaptive Coordinate Real-space Electronic Structure (ACRES) method of the terminal oxygen vacancy on the (010) surface of MoO<sub>3</sub>, within a (2 × 2) ordered array of vacancies on the surface. Analysis of the electronic structure of this surface shows that there are unoccupied dangling d<sub>xz</sub> and d<sub>z<sup>2</sup></sub> orbitals perpendicular to the surface that are created by the removal of terminal oxygen. The Mo–oxygen bonds surrounding the vacancy contract; however, the overall morphology of the surface is not drastically distorted. The vacancies alter the chemical character of the surface, as shown by studies of hydrogen and methyl binding. On both the “perfect” and vacancy surfaces, hydrogen was most strongly adsorbed over the terminal oxygen and most weakly bound over the symmetric bridging oxygen. Hydrogen is bound over the Mo atom, with a slightly smaller binding energy than hydrogen over the asymmetric bridging oxygen. The most favorable binding site for methyl on the vacancy surface is over the Mo atom exposed by removal of a terminal oxygen, whereas methyl bound to terminal oxygen is most stable on the perfect surface. There is no local minimum for adsorption over the symmetric bridging oxygen; instead, a methyl placed over this site moves toward the terminal oxygen vacancy. Analysis of the bonding shows that methyl is bound more strongly than hydrogen over the Mo atom because the C 2p orbital has better overlap with the Mo d<sub>z<sup>2</sup></sub> orbital than the hydrogen 1s. In addition, the steric repulsion observed for methyl over the perfect MoO<sub>3</sub>(010) surface is more easily relieved with the presence of the terminal oxygen vacancy.

## Introduction

The partial oxidation of methane remains one of the most important transformations for the chemical industry and heterogeneous catalysis. Methane along with other alkanes is difficult to partially oxidize because they are unreactive and thus do not readily bond to other species. The rate-limiting step in the partial oxidation process is the breaking of the first C–H bond, a process that generally requires high temperatures. An efficient catalyst must therefore combine high conversion rates with high selectivity for partial oxidation products.

Experimental studies of MoO<sub>3</sub> have attributed the activity of the catalyst to factors such as the surface structure, the nature of the oxygen species, as well as the oxidation state of the Mo.<sup>1–8</sup> MoO<sub>3</sub> is an interesting material in that it contains three distinct oxygen species, each with different coordination to Mo atoms. The terminal oxygen is doubly bound to a single Mo atom at a bond length of 1.67 Å. The asymmetric bridging

oxygen bonds to two Mo atoms with lengths of 1.79 and 2.24 Å, while the symmetric bridging oxygen is bound to three Mo atoms, with two equivalent Mo–O bonds of length 1.95 Å, and a longer bond of length 2.33 Å.<sup>9</sup>

An important issue in metal oxide catalysis is the role of surface defects in determining the activity and selectivity of the catalyst. Stoichiometric MoO<sub>3</sub> is unreactive toward methane oxidation: reduced Mo centers are necessary for any activity.<sup>1,2,5,10</sup> However, the effect that defects have on bonding and bond activation of molecular intermediates is not known. Experimentally, the structure of surface defects on MoO<sub>3</sub> has been studied with several methods, including angle-resolved ultraviolet photoemission spectroscopy<sup>11</sup> and electron diffraction.<sup>12</sup> It was found that the (010) surface is easily reduced by electron beams, which creates defect structures on the surface. An early study by Bursill of the oxygen vacancies created by exposing MoO<sub>3</sub>(010) to an electron beam reveals that shear planes in the (120) direction are formed.<sup>12</sup> For these planar defects to form, there must be oxygen vacancies along this plane. Bursill identifies an intermediate domain present prior to the formation of the shear plane in which a (7 × 7) ordered array of terminal oxygen vacancies on both the top and bottom of a MoO<sub>3</sub> layer are seen. The shear plane is then formed to eliminate these oxygen vacancies. The presence of an extended defect such as a shear plane is confirmed by a study using angle-resolved ultraviolet photoemission spectroscopy, which found that the defect state caused by oxygen deficiency showed

\* To whom correspondence should be addressed: e-mail friend@chemistry.harvard.edu.

<sup>†</sup> Department of Chemistry.

<sup>‡</sup> Department of Physics and Division of Engineering and Applied Sciences.

(1) Banares, M. A.; Fierro, J. L. G. *Catal. Lett.* **1993**, *17*, 205–211.

(2) Banares, M. A.; Rodriguez-Ramos, I.; Guerrero-Ruiz, A.; Fierro, J. L. G. *New Frontiers Catal.* **1993**, 1131–1144.

(3) Spencer, N. D. *J. Catal.* **1988**, *109*, 187–197.

(4) Smith, M. R.; Ozkan, U. S. *J. Catal.* **1993**, *142*, 226–236.

(5) Banares, M. A.; Fierro, J. L. G.; Moffat, J. B. *J. Catal.* **1993**, *142*, 406–417.

(6) Suzuki, K.; Hayakawa, T.; Shimizu, M.; Takehira, K. *Catal. Lett.* **1995**, *30*, 159–169.

(7) Smith, M. R.; Ozkan, U. S. *J. Catal.* **1993**, *141*, 124–139.

(8) Volta, J. C.; Tatibouet, J. M. *J. Catal.* **1985**, *93*, 467–470.

(9) Kihlberg, L. *Arkiv Kemi* **1963**, *21*, 357–365.

(10) Spencer, N. D.; Pereira, C. J. *AIChE J.* **1987**, *33*, 1808–1812.

(11) Firment, L. E.; Ferretti, A.; Cohen, M. R.; Merrill, R. P. *Langmuir* **1985**, *1*, 166–169.

(12) Bursill, L. A. *Proc. R. Soc. A* **1969**, *311*, 267–290.

dispersion in  $\mathbf{k}_\perp$  but not in  $\mathbf{k}_\parallel$ .<sup>11</sup> Diffusion of oxygen vacancies is important for producing the extended defect state.

Theoretically, there has been only one early study of the removal of oxygen from MoO<sub>3</sub>. This study, by Brockawik and Haber,<sup>13</sup> used small clusters of less than 10 atoms to assess the relative energetics of the terminal oxygen vacancy and the corresponding shear plane formation. The calculations, which used the X $\alpha$  method with the muffin-tin approximation, found that the removal of terminal oxygen was more favorable if accompanied by the formation of a shear plane. However, geometries were assumed for the vacancy structure as well as the shear structure, which could change the energetics considerably. Furthermore, the possible limitations of the cluster approximation, such as edge effects and the small size of the cluster, for this system are cause for concern.

The aim of this work is to explore from a theoretical perspective the role of defects on bonding of molecular intermediates to the surface. To this end, we have studied isolated terminal oxygen vacancies on MoO<sub>3</sub>(010) using density functional theory and periodic slab-configurations. Isolated oxygen vacancies may be an idealized structure that does not occur under normal conditions, but this configuration serves as a first step in the formation of more realistic defect structures. Thus, the effect of isolated vacancies on the reactivity of the surface is the natural starting point of a theoretical analysis. The use of first-principles techniques to study this problem is advantageous because it allows the explicit investigation of particular vacancy structures on the surface. The addition of hydrogen and methyl at selected sites on the vacancy-containing surface is used to probe the chemical activity of individual binding sites.

Vacancies at terminal oxygen positions were selected for study because Mo atoms, whose electronic structure is markedly different than that of oxygen, are exposed and, thus, the electronic character of the surface is expected to change. Furthermore, studies of these vacancies tests the importance of terminal oxygen for the catalytic activity of MoO<sub>3</sub>, as has been suggested by several experimental studies.<sup>7</sup> Finally, the terminal oxygen vacancy is the precursor to the formation of more extended defects such as shear planes. It is important to note that the defect structure used in these calculations is only a model for studying the isolated terminal oxygen vacancy; the experimentally observed (7 × 7) structure is currently intractable; due to the size of the calculation, we are limited to a (2 × 2) unit cell. Nevertheless, our model system will yield valuable insight into the nature of point defects on the MoO<sub>3</sub> surface under conditions where the concentration of defects is relatively small.

Hydrogen and methyl are used as probes to model the interactions at the surface after initial C–H bond breaking of methane. Specifically, comparison can be made to the adsorption of hydrogen and methyl on the perfect MoO<sub>3</sub>(010) surface to gauge the effect of surface defects. This study examines the effect of defects on the adsorption of hydrogen and methyl on the MoO<sub>3</sub> surface, and therefore provides information about the favored configuration of products following methane dissociation.

## Computational Details

All calculations were performed by using density functional theory in the local density approximation with pseudopotentials to represent the core states. The Kohn–Sham equations were solved in real space

with use of the Adaptive Coordinate Real-Space (ACRES) code,<sup>14–16</sup> which is an electronic structure code optimized for parallel platforms. Although the code can be used with an adaptive mesh, a regular grid was used in this work because the pseudopotentials for all species involved here have nearly equivalent features, requiring the same level of grid resolution. The grid spacing was chosen so as to give an equivalent cutoff of 60 Ry for a plane-wave basis. The electron density was relaxed by using Pulay mixing,<sup>17,18</sup> and the Hamiltonian was diagonalized by using a modified Lanczos scheme. The optimized norm-conserving pseudopotential for Mo including states up to 4d was generated with  $r_{c,s} = r_{c,p} = r_{c,d} = 1.7$  au from a singly ionized reference configuration of [Kr]4s<sup>2</sup>4p<sup>6</sup>4d<sup>5</sup> and is expressed in the fully separable Kleinman–Bylander form.<sup>19</sup> Optimization<sup>20</sup> was performed with  $q_{c,s} = q_{c,d} = 6.5$  Ry<sup>1/2</sup> and  $q_{c,p} = 7.5$  Ry<sup>1/2</sup> and 6, 4, and 4 Bessel functions for the s, p, and d orbitals, respectively. The soft oxygen pseudopotential was generated according to the scheme of Troullier and Martins<sup>21</sup> with core radii  $r_{c,s} = 1.3$  and  $r_{c,p} = 1.65$  au. An optimized norm-conserving pseudopotential was also used for C, with core radii  $r_{c,s} = 1.0$  and  $r_{c,p} = r_{c,d} = 1.4$  au. These pseudopotentials have been tested in previously published work on the MoO<sub>3</sub>(010) surface.<sup>22</sup>

The MoO<sub>3</sub> surface was modeled by one layer of the bulk structure with the surface perpendicular to the (010) direction, an approximation that is expected to be excellent because of weak interlayer coupling. This model has been tested previously,<sup>22</sup> and yields bond lengths and vibrational frequencies in excellent agreement with experimental values. A (2 × 2) array of terminal oxygen vacancies was created, corresponding to a unit cell size four times that of the perfect surface. This layer was repeated with experimental bulk lattice constants in the directions parallel to the surface, and with 14 Å of vacuum between layers. The Brillouin zone was sampled at the  $\Gamma$  point for all calculations. Hydrogen and methyl were placed over possible binding sites on the MoO<sub>3</sub>(010) surface with terminal oxygen vacancies and the ionic positions were relaxed until the RMS force was less than 0.005 au/Å.

To elucidate the importance of individual orbital contribution to bonds, the crystal orbital overlap population (COOP) was used.<sup>23</sup> The COOP is a projection of two individual atomic orbitals onto a crystal wave function, weighted by the overlap of the two atomic orbitals. The sign of the COOP is an indication of the bonding or antibonding contribution of the two orbitals to the crystal wave function, and the magnitude is indicative of the strength of the interaction. Thus, the COOP can be used as a more specific indicator of the nature of covalent bonding in the system.

## Results

**MoO<sub>3</sub>(010) with Terminal Oxygen Vacancy.** The formation of a vacancy on the MoO<sub>3</sub>(010) surface by removal of a terminal oxygen does not significantly alter the surface structure. Changes are localized around the Mo vacancy such that Mo is pulled toward the oxygen below and the surrounding oxygens move closer to the Mo vacancy site (Figure 1, Table 1). The oxygen atoms originally at the adjacent symmetric bridging site are no longer symmetrically bound in the presence of the vacancy. Rather, the oxygen is bound more closely to the Mo atom containing the vacancy, such that their bond lengths in the presence of the vacancy become 1.90 and 1.96 Å, compared to

(14) Modine, N. A.; Zumbach, G.; Kaxiras, E. *MRS Symp. Proc.* **1996**, 408, 139.

(15) Zumbach, G.; Modine, N. A.; Kaxiras, E. *Solid State Comm.* **1996**, 99, 57–61.

(16) Modine, M. A.; Zumbach, G.; Kaxiras, E. *Phys. Rev. B* **1997**, 55, 10289–10301.

(17) Kresse, G.; Furthmüller, J. *Phys. Rev. B* **1996**, 54, 11169–11186.

(18) Kresse, G.; Furthmüller, J. *Comput. Mater. Sci.* **1996**, 6, 15–50.

(19) Kleinman, L.; Bylander, D. M. *Phys. Rev. Lett.* **1982**, 48, 1425.

(20) Rappe, A. M.; Rabe, K. M.; Kaxiras, E.; Joannopoulos, J. D. *Phys. Rev. B* **1990**, 41, 1227.

(21) Troullier, N.; Martins, J. L. *Phys. Rev. B* **1991**, 43, 1993.

(22) Chen, M.; Waghmare, U. V.; Friend, C. M.; Kaxiras, E. *J. Chem. Phys.* **1998**, 109, 6854–6860.

(23) Hoffmann, R. *Solids and Surfaces: A Chemist's View of Bonding in Extended Structures*; VCH Publishers: New York, 1988.

(13) Broclawik, E.; Haber, J. *J. Catal.* **1981**, 72, 379–382.

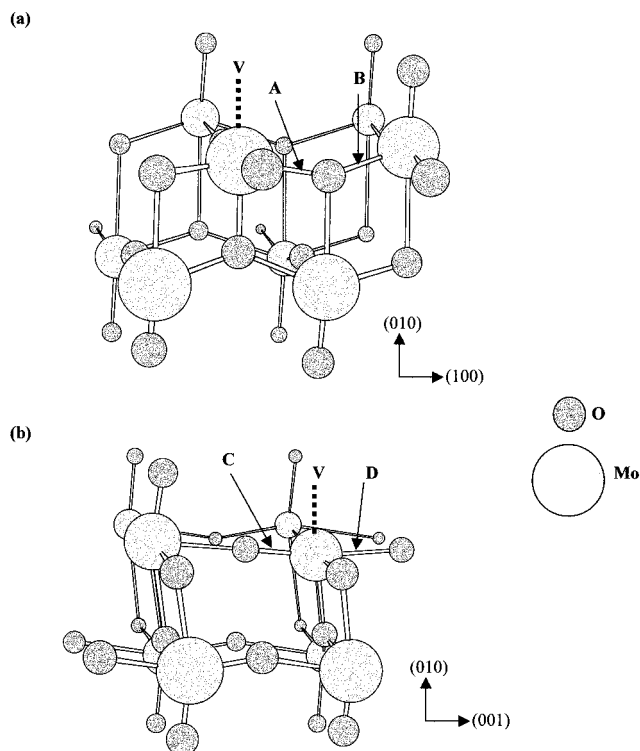


**Figure 1.** Schematic of the  $\text{MoO}_3(010)$  surface with a  $(2 \times 2)$  array of terminal oxygen vacancies (V indicates the position of the missing oxygen atom, other letters refer to bond lengths tabulated in Table 1): (a)  $\text{MoO}_3(010)$  surface with terminal oxygen vacancy, view of the symmetric bridging oxygen, and (b)  $\text{MoO}_3(010)$  surface with terminal oxygen vacancy, view of the asymmetric bridging oxygen.

**Table 1.** Bond Lengths of  $\text{MoO}_3(010)$  with Terminal Oxygen Vacancy

type of oxygen	$\text{MoO}_3(010)$ w/ vacancy <sup>a</sup>	"perfect" $\text{MoO}_3(010)$
asymmetric bridging O	1.72 (C) 2.08 (D)	1.79 2.33
symmetric bridging O	1.90 (A) 1.96 (B)	1.95 1.95

<sup>a</sup> The letters after the bond lengths refer to the bonds indicated in Figure 1.

equivalent bonds of 1.95 Å in the perfect surface. Similarly, the asymmetric bridging oxygen is bound to the Mo atom containing the vacancy by a bond length of 1.72 Å, compared to a bond length of 1.79 Å on perfect  $\text{MoO}_3(010)$ . The lengths of the Mo–O bonds adjacent to the vacancy remain close to their unperturbed values, indicating that there is minimal interaction between vacancies in neighboring unit cells for the  $(2 \times 2)$  array.

Examination of the energy spectrum of the  $\text{MoO}_3$  surface with terminal oxygen vacancies reveals a new state that is located in the band gap (Figure 2). This state is a  $d_{xz}$  nonbonding state of Mo that is localized on the Mo atom to which the missing O was bonded, as can be seen by plotting this orbital (Figure 3a). There is also a "dangling"  $d_z^2$  state in the conduction band that is localized on the Mo atom and directed perpendicular to the surface (Figure 3b). The energetic cost of removing one out of every four terminal oxygen atoms is 10.1 eV, and is calculated by subtracting the total energy of the perfect surface from the sum of energies of the vacancy surface and a free oxygen atom. A comparison can be made to the cost of simply removing the terminal oxygen, without allowing any relaxation of the surface; this value is calculated to be 13.4 eV. Therefore,

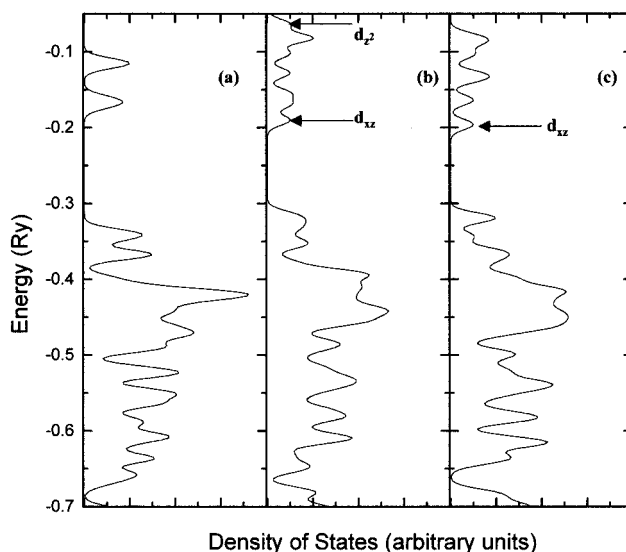


**Figure 2.** Density of states plots (only states near the band gap are shown): (a) "Perfect"  $\text{MoO}_3(010)$  surface; (b)  $\text{MoO}_3(010)$  surface with a  $(2 \times 2)$  array of terminal oxygen vacancies. The symbols  $d_{xz}$  and  $d_z^2$  indicate the energy of individual orbitals related to the creation of the vacancy and (c) hydrogen adsorbed over the terminal oxygen vacancy.

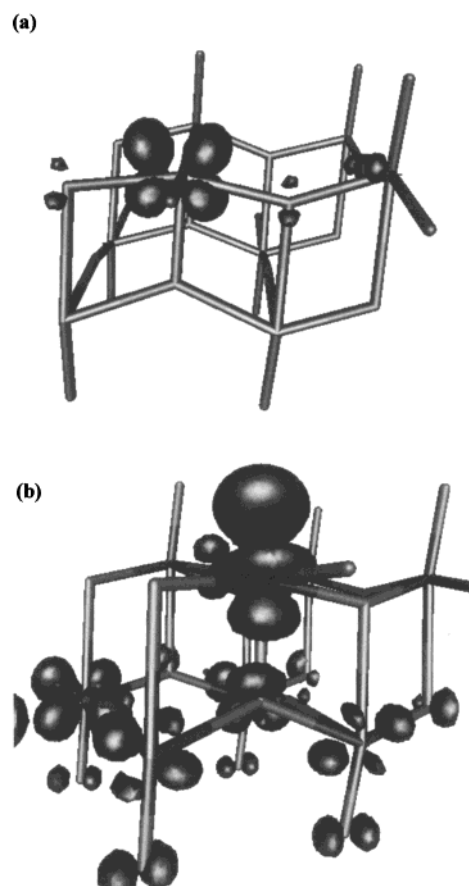


**Figure 3.** Isoelectronic plots of vacancy-localized states (see Figure 2b for the corresponding position in the density of states): (a)  $d_{xz}$  orbital and (b)  $d_z^2$  orbital.

the relaxation of the surface after the removal of a terminal oxygen accounts for a 3.3 eV lowering in energy.

**Site-Dependent Binding of H to  $\text{MoO}_3(010)-(2 \times 2)-v$ .** Hydrogen atom binding to different sites on  $\text{MoO}_3(010)$  with a  $(2 \times 2)$  array of terminal oxygen vacancies was studied to examine site-dependent bonding and stability. In particular,



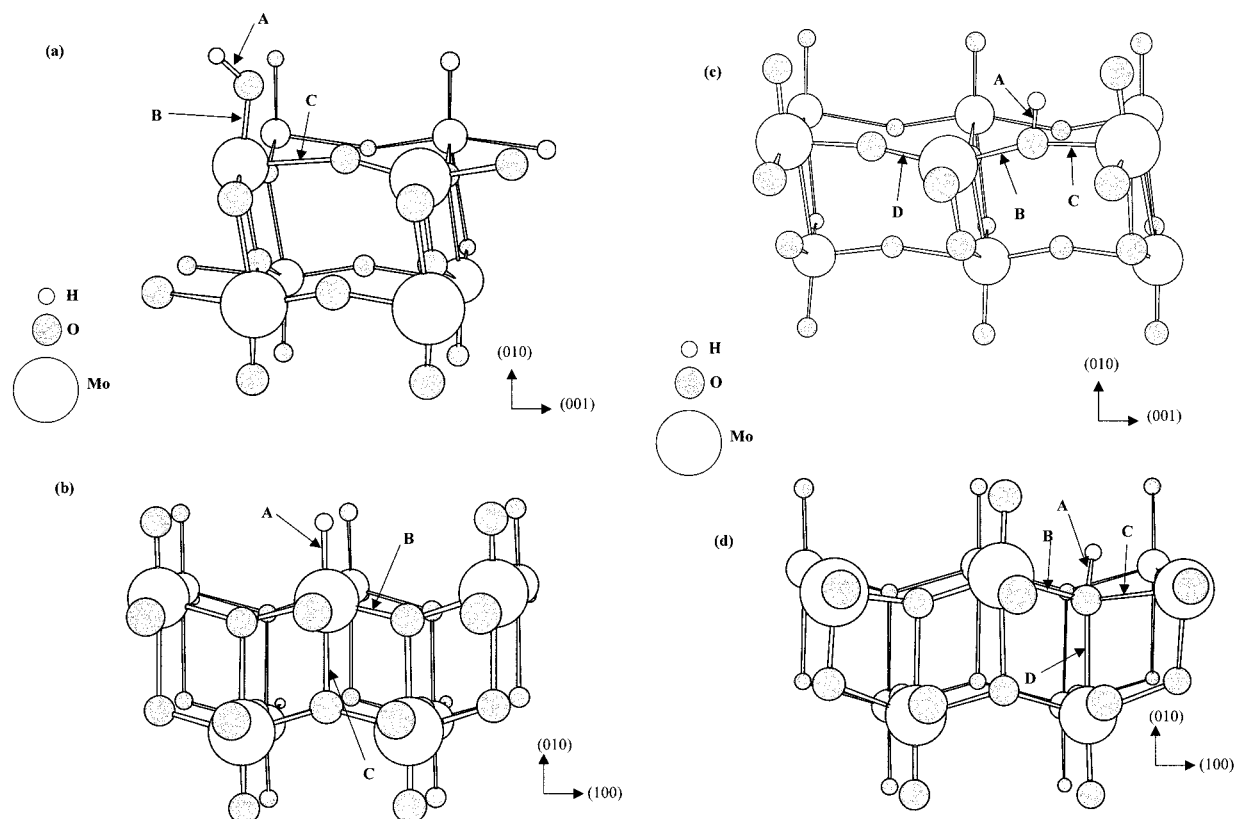


**Figure 4.** Schematic of the lowest energy configurations for hydrogen bound to various sites on the  $\text{MoO}_3(010)$  surface with a  $(2 \times 2)$  array of terminal oxygen vacancies. Shown is hydrogen bound to (a) terminal oxygen, (b) the vacancy, (c) symmetric bridging oxygen, and (d) the asymmetric bridging oxygen. The most energetically favorable site is for hydrogen bound to the terminal site ( $-4.4$  eV) with binding to the asymmetric bridge site close in energy ( $-4.1$  eV).

**Table 2.** Binding Energies for Hydrogen and Methyl Adsorbed on Different Binding Sites of the  $\text{MoO}_3(010)$  Surface with a  $(2 \times 2)$  Array of Terminal Oxygen Vacancies

binding site	energy (eV)	
	hydrogen	methyl
terminal oxygen vacancy	$-3.8$	$-4.0$
terminal oxygen	$-4.4$	$-3.9$
asymmetric bridging oxygen	$-4.1$	$-3.7$
symmetric bridging oxygen	$-2.0$	

hydrogen over the Mo atom next to the terminal oxygen vacancy, the bridging oxygens adjacent to the vacancy, and the neighboring terminal oxygen were considered to find the most favorable binding site (Table 2). Only oxygen sites adjacent to the vacancy were tested, as all other oxygens had bond lengths close to those in the “perfect” surface.

Hydrogen is most weakly bound over the symmetric bridging oxygen, with a binding energy of  $-2.0$  eV. Hydrogens bound to the other sites—the vacancy, the asymmetric bridging oxygen, and the terminal oxygen—have similar binding energies,  $-3.8$ ,  $-4.1$ , and  $-4.4$  eV, respectively. The Mo–terminal oxygen bond is lengthened by  $0.13$  Å to  $1.80$  Å upon adsorption of hydrogen, similar to the perfect  $\text{MoO}_3(010)$  surface (Figure 4, Table 3).

Hydrogen is bound to the vacancy primarily via the previously dangling  $d_{z^2}$  orbital of the Mo. This assertion is based on the fact that the vacancy state in the gap corresponding to the nonbonding Mo  $d_{xz}$  orbital is still present in the density of states following binding of hydrogen to the vacancy (Figure 2c). The Mo  $d_{z^2}$  peak in the density of states moves to lower energy through interaction with the hydrogen and no longer appears in the conduction band (Figure 2c). The hydrogen does not

**Table 3.** Selected Bond Lengths for Hydrogen Adsorbed on Different Binding Sites of the  $\text{MoO}_3(010)$  Surface with a  $(2 \times 2)$  Array of Terminal Oxygen Vacancies (see Figure 4 for bond designations, which are different for each binding site; all bond lengths in Å)

bond	binding site			
	terminal O	vacancy	asym bridging O	sym bridging O
A	0.97	1.73	0.98	1.03
B	1.80	1.87	2.03	1.95
C	2.33	2.34	2.18	2.03
D	-	-	1.80	2.42

compensate fully for the reduced bonding due to the missing terminal oxygen, however, because the Mo–O bond lengths of the oxygens surrounding the Mo atom adjacent to the vacancy are still shortened relative to the perfect surface. The hydrogen is actually bound with a bond length that is greater than the terminal oxygen,  $1.72$  Å vs  $1.67$  Å (Figure 4, Table 3). With some bonding between the asymmetric oxygen and the Mo atom depleted by oxygen bonding to hydrogen, which is indicated by an increase in the Mo–O bond length from  $1.72$  to  $2.03$  Å, the Mo pulls the other asymmetric bridging oxygen even closer, to a bond length of  $1.80$  Å, from its value of  $2.08$  Å on the clean vacancy surface (Figure 4, Table 3). Finally, hydrogen bound to the symmetric bridging oxygen causes some surface relaxation. The symmetric bridging oxygen moves upward perpendicular to the surface by about  $0.06$  Å, weakening its long bond with the Mo beneath (Figure 4, Table 3).

**Site-Dependent Binding of Methyl to  $\text{MoO}_3(010)-(2 \times 2)-v$ .** Methyl is the most strongly bound to the exposed Mo atom created by the removal of a terminal oxygen (Table 2). The C–Mo distance is  $2.00$  Å, with corresponding C–H bond

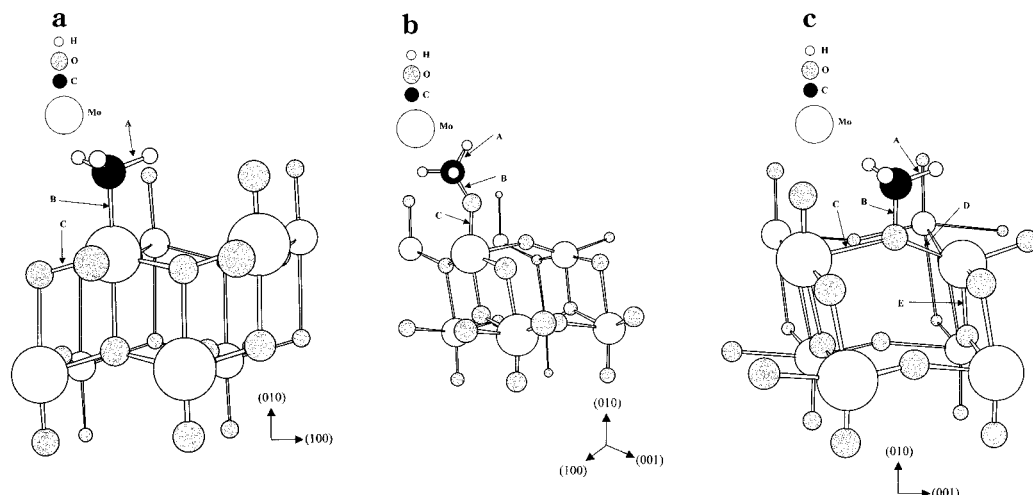


**Figure 5.** Scale models of the minimum energy configurations of methyl bound to various surface sites on the  $\text{MoO}_3(010)$  surface with a  $(2 \times 2)$  array of terminal oxygen vacancies. Shown is methyl bound to (a) the vacancy, (b) terminal oxygen, and (c) asymmetric bridging oxygen. The vacancy site is most stable ( $-4.0$  eV); however, the terminal oxygen site has a similar binding energy ( $-3.9$  eV). There is no energy minimum for methyl bound to the symmetric oxygen.

lengths of  $1.1 \text{ \AA}$  (Figure 5a, Table 4). The Mo–C–H bond angle is  $109.34^\circ$ , which is extremely close to the perfect tetrahedral angle. This indicates that there is little interaction between the Mo atom and the C–H orbitals, unlike methyl adsorbed on metal surfaces.<sup>24–26</sup>

The adsorption of methyl on the terminal vacancy also restores the bond lengths of some of the Mo–O bonds toward the values for perfect  $\text{MoO}_3(010)$ . For example, the symmetric bridging O–Mo bond lengths next to the methyl remain approximately the same as on the vacancy surface, at  $1.88 \text{ \AA}$ . The asymmetric bridging oxygens are bound to the Mo with methyl adsorbed with bond lengths of  $1.73$  and  $2.14 \text{ \AA}$ , compared to  $1.72$  and  $2.08 \text{ \AA}$  on  $\text{MoO}_3(010)-(2 \times 2)-v$  and  $1.75$  and  $2.24 \text{ \AA}$  on perfect  $\text{MoO}_3(010)$ .

Methyl binds to terminal oxygen to form methoxy with an energy that is  $0.19$  eV higher in energy than over the Mo atom. The binding of methyl to the terminal oxygen lengthens the Mo–O bond from  $1.67$  to  $1.79 \text{ \AA}$ , as the bond changes from a double to a single bond, as compared with a value of  $1.86 \text{ \AA}$  when  $0.5$  ML of methyl is bound to the  $\text{Mo}=\text{O}$  site on the perfect surface (Figure 5b, Table 4).<sup>27</sup> The C–O and C–H bond lengths,  $1.39$  and  $1.10 \text{ \AA}$ , respectively, are identical with the analogous bond lengths for methyl adsorbed on the perfect  $\text{MoO}_3(010)$  surface.

Methyl bound to the asymmetric bridging oxygen is  $0.32$  eV less stable than over the terminal oxygen vacancy. The methyl pulls the asymmetric bridging oxygen out of the surface by  $0.24 \text{ \AA}$  so that the oxygen is bonded to the two Mo atoms with bond lengths of  $1.94$  and  $2.44 \text{ \AA}$ , which is qualitatively similar to the relaxation seen over the perfect surface when methyl is adsorbed over the analogous site (Figure 5c, Table 4). The C–O bond length is  $1.41 \text{ \AA}$ , and the C–H bond lengths are  $1.10 \text{ \AA}$ , almost identical with the bond lengths found for methyl adsorbed on the asymmetric bridging oxygen for the perfect surface. Finally, methyl was also placed over the symmetric bridging oxygen; however, there was no energy minimum directly above the symmetric bridging oxygen. Instead, the methyl moved

**Table 4.** Selected Bond Lengths for Methyl Adsorbed on Different Binding Sites of the  $\text{MoO}_3(010)$  Surface with a  $(2 \times 2)$  Array of Terminal Oxygen Vacancies (see Figure 5 for bond designations, which are different for each binding site; all bond lengths in  $\text{Å}$ )

bond	binding site		
	vacancy	terminal O	asym bridging O
A	1.10	1.10	1.10
B	2.02	1.40	1.41
C	1.88	1.80	2.45
D	-	-	1.94
E	-	-	1.88

toward the Mo atom until it was bound directly over the terminal oxygen vacancy.

## Discussion

We have identified two vacancy-localized states, a Mo  $d_{xz}$  orbital which appears in the band gap and a Mo  $d_z^2$  orbital that is located in the conduction band, that are important in determining the chemical characteristics of point defects at  $\text{Mo}=\text{O}$  sites in  $\text{MoO}_3$ . The Mo is bound to the terminal oxygen through interactions of these two Mo 4d orbitals with O 2p orbitals. A  $\sigma$  bond is formed from the overlap of the Mo  $d_z^2$  orbital with the  $2p_z$  orbital of oxygen. The interaction of the Mo 4d<sub>xz</sub> orbital with the O  $2p_x$  orbital yields a  $\sigma$  bond.

These two orbitals are responsible for bonding adsorbates to the Mo atom. The  $d_z^2$  orbital forms  $\sigma$  bonds while the  $d_{xz}$  orbital forms  $\pi$  bonds. For the adsorbates studied here, the main interaction is through the  $d_z^2$  orbital; however, for bonding molecules such as CO or NO the  $d_{xz}$  orbital plays a larger role in the binding.<sup>28</sup> Nevertheless, there are differences in adsorbate binding even to the  $d_z^2$  orbital, as the case of hydrogen and methyl illustrates.

Methyl adsorbed over the  $\text{MoO}_3(010)$  surface with an ordered  $(2 \times 2)$  array of terminal oxygen vacancies is most strongly bound at the vacancy site, whereas hydrogen is most stable over the terminal oxygen. This difference can be explained by closely analyzing the bonding between H and  $\text{CH}_3$  to the different sites. We find that the main difference lies in the amount of overlap between the Mo  $4d_z^2$  orbital and the adsorbate orbitals.

(24) Chen, M.; Friend, C. M.; van Santen, R. A. *Catal. Today* **1999**, *50*, 621–627.

(25) Kratzer, P.; Hammer, B.; Nørskov, J. K. *J. Chem. Phys.* **1996**, *105*, 5595–5604.

(26) Yang, H.; Whitten, J. L. *Surf. Sci.* **1991**, *255*, 193–207.

(27) Chen, M.; Friend, C. M.; Kaxiras, E. K. *J. Chem. Phys.* **1999**, *112*, 9617–9623.

(28) Chen, M.; Friend, C. M.; Kaxiras, E. K. *J. Chem. Phys.* In preparation.

**Table 5.** OPDOS for Methyl and Hydrogen Adsorbed on Selected Binding Sites of MoO<sub>3</sub>(010) with a (2 × 2) Array of Terminal Oxygen Vacancies

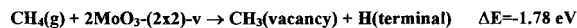
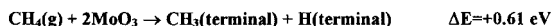
adsorbate	orbitals	OPDOS
CH <sub>3</sub> over terminal O	Mo 4d-terminal O 2p	0.14
CH <sub>3</sub> over Mo	C 1sp-Mo d	0.22
H over terminal O	Mo 4d-terminal O 2p	0.14
H over Mo	H 1s-Mo 4d	0.12

In comparing the binding of methyl vs hydrogen to a Mo atom, differences in bonding are expected because of the higher degree of localization and directionality of the d orbitals. This is indeed evident in the analysis of methyl–Mo and H–Mo bonding. The overlap population density of states (OPDOS) for the Mo 4d–C 2sp interaction is calculated to be 0.22 (Table 5), while for the Mo 4d–H 1s interaction the value is 0.13. The bonding in this case favors the directional bonding of the methyl sp<sup>3</sup> hybrid orbital over the nondirectional hydrogen 1s orbital. The directed orbitals for both Mo and methyl allow for better overlap than the hydrogen 1s orbital. Therefore, the hydrogen 1s orbital has a stronger bonding interaction with the terminal oxygen 2p orbital than with the Mo 4d<sub>z<sup>2</sup></sub> orbital. It is this difference in Mo–methyl bonding vs Mo–H bonding that determines the overall energy ordering of adsorption sites for methyl vs hydrogen on the vacancy surface.

Both methyl and hydrogen weaken the Mo–terminal O bond equally when adsorbed onto the terminal oxygen site. A crystal orbital overlap population (COOP) analysis on the terminal O 2p–Mo 4d interaction when methyl is adsorbed to the terminal oxygen yields an OPDOS of 0.14, where the OPDOS refers to the COOP summed to the Fermi level. The equivalent calculation between the terminal O 2p–Mo 4d orbitals for hydrogen adsorbed over the terminal oxygen gives the same value of 0.14 for the OPDOS (Table 5). This indicates that the Mo–terminal O bond is weakened in the same manner whether methyl or hydrogen is adsorbed to the terminal site. This is further substantiated by the Mo–terminal O bond length, which is 1.80 Å with methyl adsorbed, compared to an almost identical 1.79 Å when hydrogen is bound to the terminal oxygen.

The differences in methyl and hydrogen binding have implications for methyl addition to an oxide surface containing terminal oxygen vacancies. The formation of methoxy by addition of methyl to the asymmetric bridging oxygen is stabilized relative to the perfect surface because the steric repulsion is lessened by the absence of one terminal oxygen. Furthermore, the terminal oxygen vacancy creates a binding site over a bare Mo atom that is more stable for methyl adsorption than the terminal oxygen site. While the terminal oxygen vacancy is necessary energetically for methane dissociation, a methyl created as a result of methane activation could end up bound to the Mo atom. If this were to occur, the terminal oxygen vacancy would be a “dead end” in oxidation reactions, since methyl bound to this site does not go on to form oxidation products. Another possibility is that at higher temperatures methyl is initially bound over the Mo atom but is able to migrate to other sites, such as over the terminal oxygen or the asymmetric bridging oxygen, where it then goes on to form the oxidation products. On the other hand, the terminal oxygen vacancy may play a role in other parts of the oxidation process; for example, the defect could be important in breaking the first C–H bond of methane. This is one aspect that was not addressed in these calculations, but which merits further study.

We can also use the binding energies of H and methyl to the vacancy surface to compare the energetics for methane dissociation to the “perfect” surface (Scheme 1). We consider the

**Scheme 1.** Energetics of Methane Dissociation**Vacancy surface****Perfect Surface**

reaction for methane dissociating into CH<sub>3</sub> and H, both bound to their most favorable binding sites. For the vacancy surface, this means methyl bound to the Mo atom and H bound to the terminal oxygen, while for the perfect surface both methyl and hydrogen are bound separately to terminal oxygens. In accordance with experimental results, the vacancy surface is energetically more favorable for methane dissociation. On the vacancy surface, this reaction is exothermic by –1.78 eV, while the same reaction on the perfect surface is endothermic by 0.61 eV. These results are in qualitative agreement with earlier semiempirical cluster calculations of methane dissociation on MoO<sub>3</sub> surfaces. Both Mehandru et al.<sup>29</sup> and Irigoyen et al.<sup>30</sup> predict better binding of methyl to a bare Mo atom than to an oxygen species. Mehandru et al. examined the effect of surface electron–hole pairs on the energetics of methane dissociation, an aspect that we do not consider here. They found that dissociation of methane to methyl that is bound to Mo and hydrogen that is bound to the terminal oxygen was slightly exothermic. On the other hand, dissociation of methane to form methyl bound to terminal oxygen and hydrogen bound to a Mo atom was energetically unfavorable, in agreement with our calculations. Irigoyen et al. consider methane dissociation on the MoO<sub>3</sub>(100) surface based on a combination of methyl and hydrogen adsorption. Similarly, these authors also find that dissociation of methane to methyl adsorbed on a Mo atom and hydrogen adsorbed on a terminal oxygen is slightly favorable.

It must be noted that all the structures and energies obtained in these calculations refer to thermodynamic minima only. At finite temperatures, there could be kinetic factors which affect the ability of a system to access the thermodynamic limits. Molecular dynamics calculations at finite temperatures are needed to assess the relative importance of thermodynamics versus kinetics.

**Conclusions**

The present density functional theory calculations of a terminal oxygen vacancy on the MoO<sub>3</sub>(010) surface indicate that the formation of the vacancy does not significantly affect the morphology of the surface. Instead, there is some surface relaxation resulting in contracted bond lengths between the Mo with the missing terminal oxygen and its surrounding oxygen atoms, in response to the missing Mo–terminal oxygen bond. The formation of the vacancy leaves dangling d<sub>xy</sub> and d<sub>z<sup>2</sup></sub> orbitals on the Mo that are able to bond to adsorbates. While methyl is most strongly adsorbed over the bare Mo atom exposed as a result of removing a terminal oxygen, hydrogen prefers to bind over the terminal oxygen. Over the symmetric bridging oxygen, there is no stable binding site for methyl; instead, methyl moves toward the exposed Mo atom. The methyl group is not significantly perturbed by adsorption on any of the binding sites, as the bond lengths and angles remain identical to gas-phase values. A comparison of adsorbed hydrogen versus adsorbed methyl shows that the directional orbitals of methyl allow better

(29) Mehandru, S. P.; Anderson, A. B.; Brazdil, J. F.; Grasselli, R. K. *J. Phys. Chem.* **1987**, *91*, 2930–2934.

(30) Irigoyen, B.; Castellani, N.; Juan, A. *J. Mol. Catal.* **1998**, *129*, 297–310.

interaction with Mo d orbitals compared to the hydrogen, explaining the different energetic order of adsorption sites. Therefore, terminal oxygen vacancies could act as “sinks” for methyl in partial oxidation reactions, although the vacancies may play other roles in different steps of the process.

**Acknowledgment.** The authors are grateful for support from Ryoka Systems, Inc., the DoD CHSSI project, and the ASC and ARL MSRC.

JA994376S